GPS radio occultation measurements on ionospheric electron density and vTEC from low Earth orbit

Lung-Chih Tsai [1, 2] ,

C. H. Liu[3], J. Y. Hyang[1], and K. Kevin Cheng[4]

(1) Center for Space and Remote Sensing research, National Central Univ. (NCU), Chung-Li, Taiwan (lctsai@csrsr.ncu.edu.tw)
(2) Institute of Space Science, NCU, Chung-Li, Taiwan
(3) Academia Sinica, Taiwan
(4) Earth and Environmental Sciences, NCCU, Chia-Yi,Taiwan

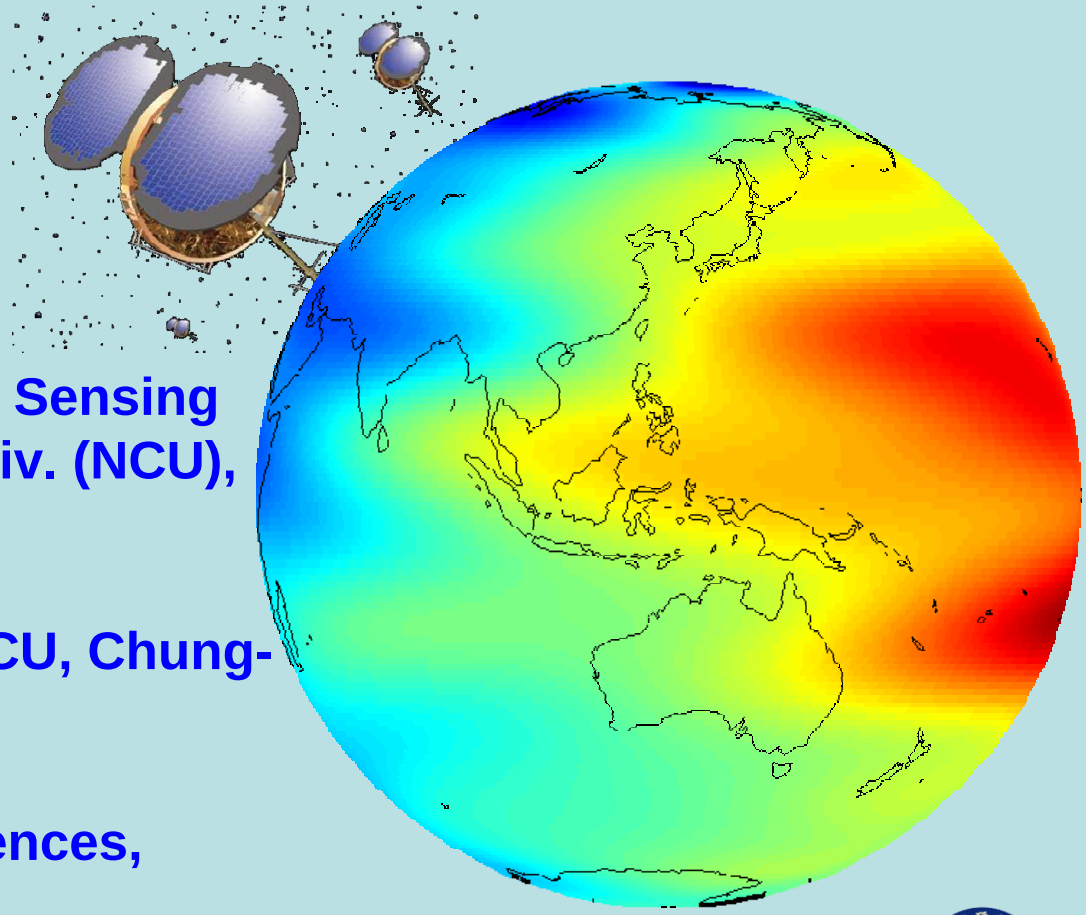

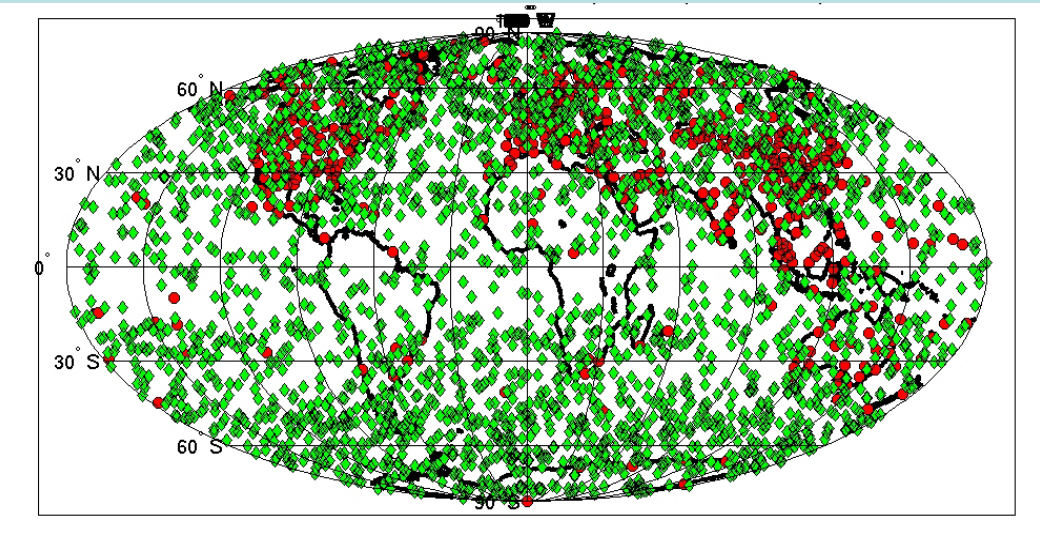

FormoSat-3 (FS3) /COSMIC: ~ 2500 radio occultation (RO) measurements worldwide daily

Numbers of daily RO observations on board FS3 / COSMIC and retrieved N_e profiles

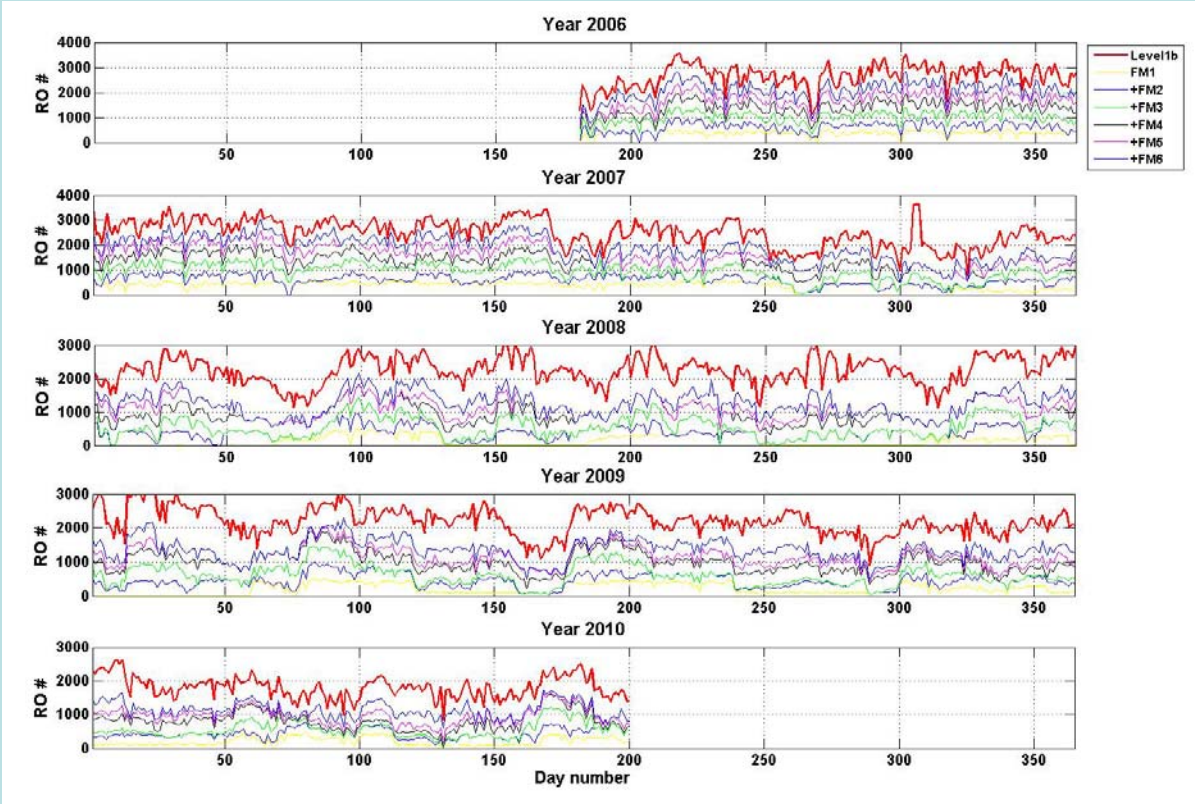

Top level view of FS3/COSMIC ionospheric data processing

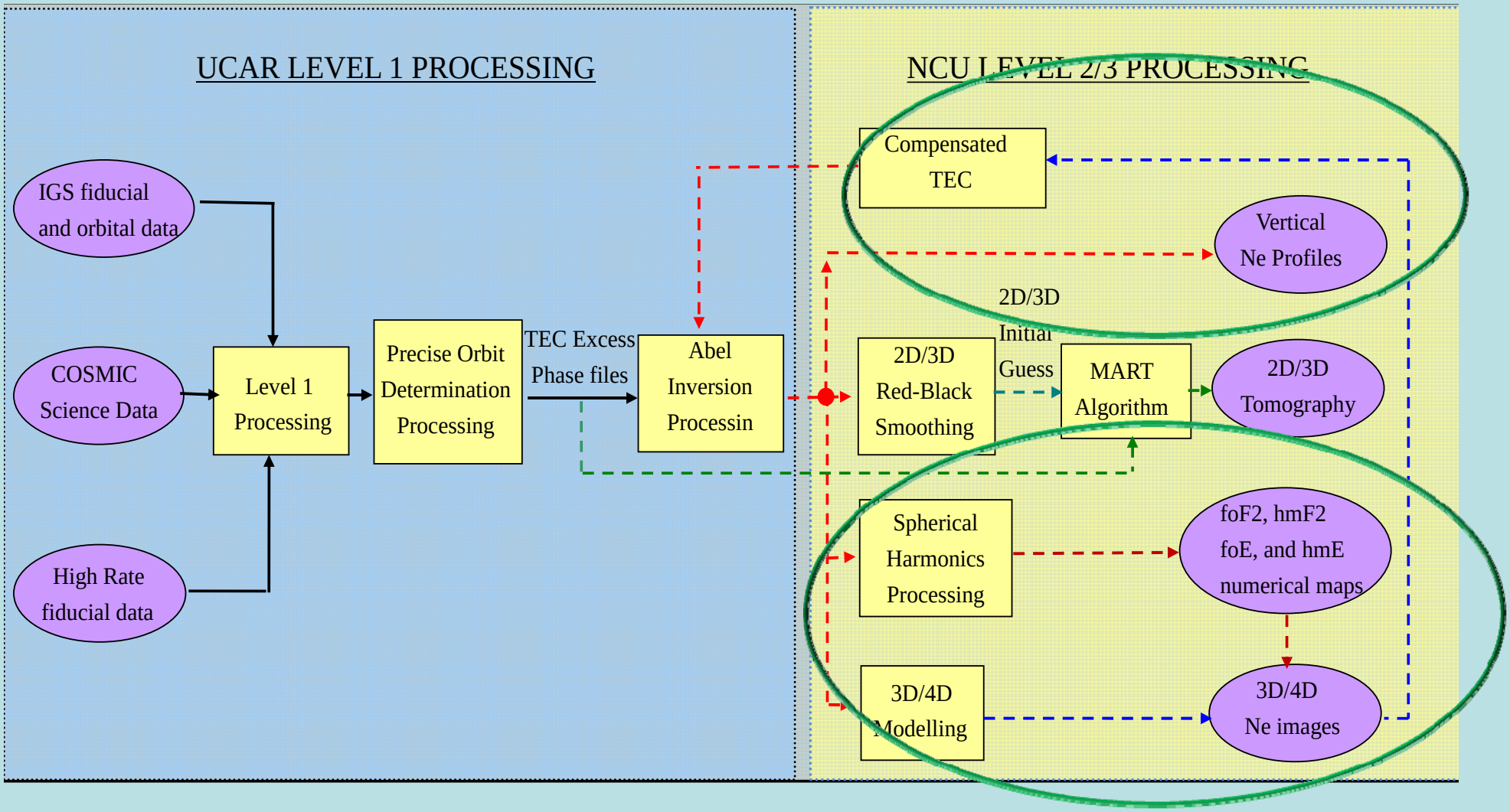

GPS RO TEC observations and vertical N_e retrieval

Assuming locally spherical symmetry of the ionospheric N_e and straight-line propagation for the GPS L1 and L2 signals:

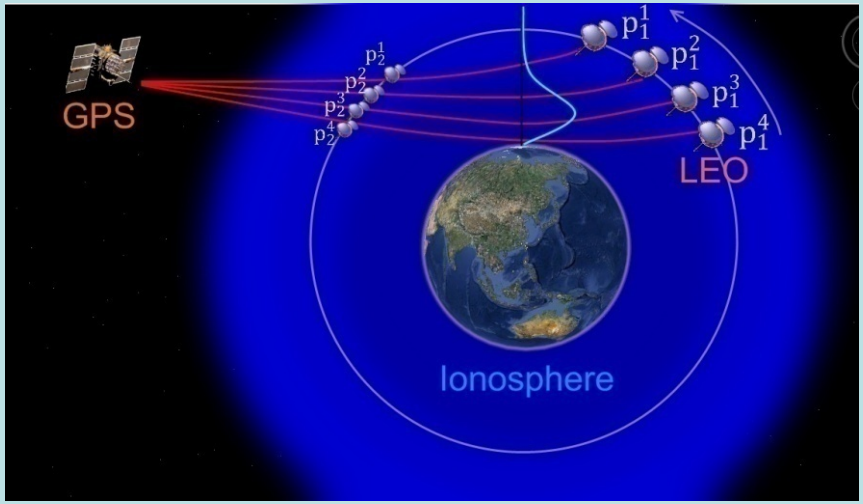

1. Calibrated TEC determination (TEC')

$$TEC'(r_t) = pTEC(P_1(r_t)) - pTEC(P_2(r_t)) \cong 2\int_{r_t}^{r_{LEO}} \frac{r\,N_e(r)}{\sqrt{r^2 - r_t^2}}\,dr\,.$$

where *pTEC*s are the path TECs from GPS to LEO, and P1 and P2 are the occulting and auxiliary positions during a GPS RO observation.

2. The Abel inversion through calibrated TECs

$$N_e(r_t) = -\frac{1}{\pi}\int_{r_t}^{r_{LEO}} \frac{d\,TEC'(r)/dr}{\sqrt{r^2 - r_t^2}}\,dr\,.$$

Example calibrated TECs (in green) and resulting N_es (in red)

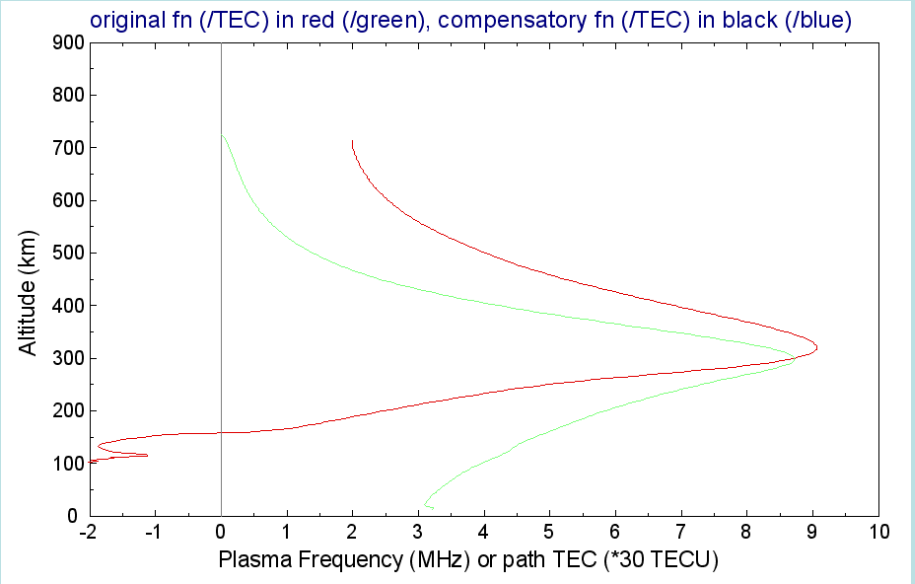

N_e retrieval errors applying the Abel inversion on TECs

- caused by the spherical symmetry assumption
- caused by the straight-line propagation (neglecting L1 & L2 ray bending) assumption
- caused by the assumption of stationary ionosphere during each occultation observation (averagely ~15 minutes)
- inadequate initial (LEO orbital) N_e and initial N_e variation below the LEO altitude
- caused by the ellipsoidal shape of the Earth
- others

Improved Abel inversion based on compensated TECs

- Compensated TEC determination (TEC*) :

$$TEC^*(r) = TEC'(r) + \int_{P_1}^{P_2'} \left(N_e^{model}(r, \theta_t(r), \lambda_t(r)) - N_e^{model}(r, \theta, \lambda) \right) dl$$

where $(r, \theta_t(r), \lambda_t(r))$ is the corresponding tangent-point position with the same radial distance along a ray.

- The Abel inversion through compensated TECs :

$$N_e^*(r_t) = -\frac{1}{\pi} \int_{r_t}^{r_{LEO}} \frac{dTEC^*(r)/dr}{\sqrt{r^2 - r_t^2}} dr$$

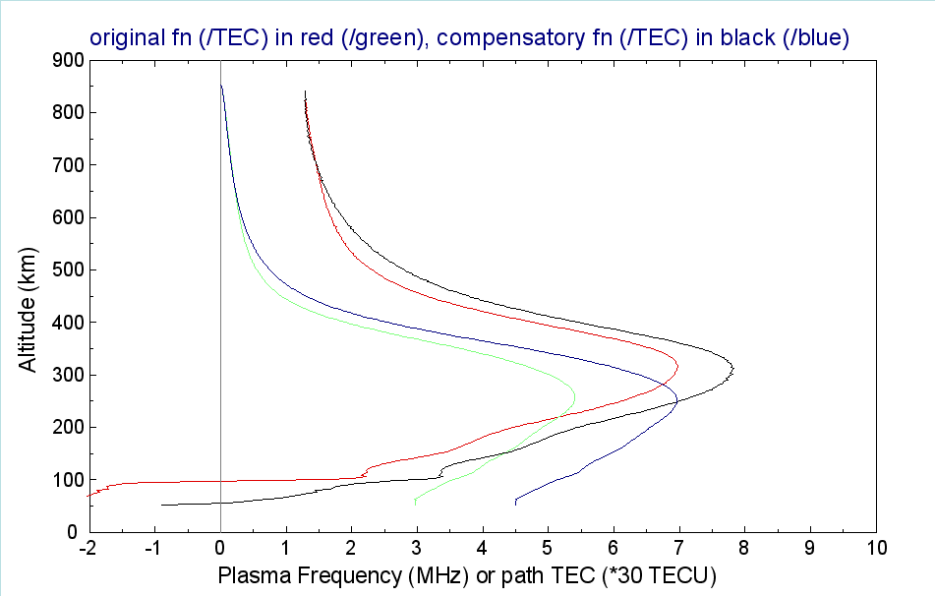

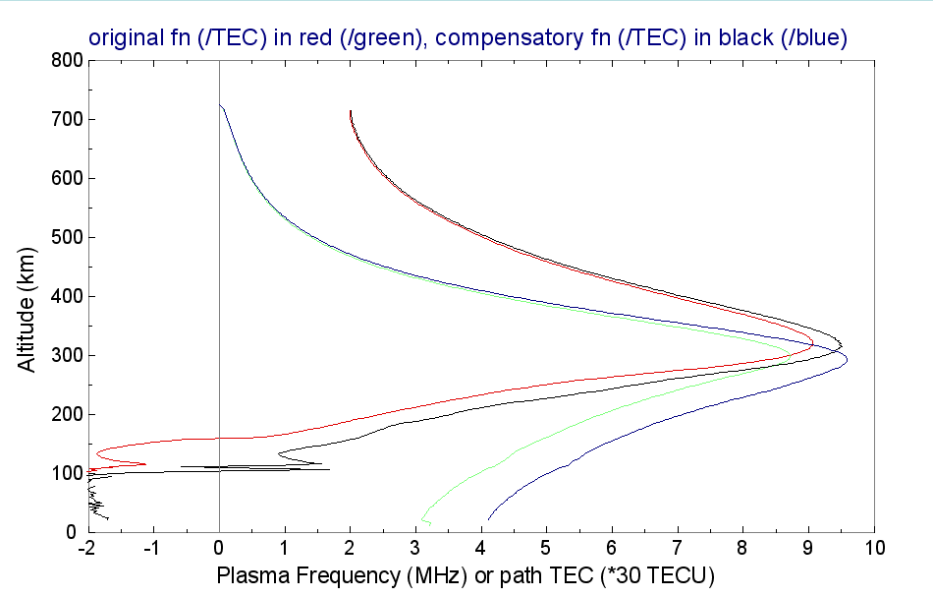

Modelling of 3D Ionospheric Electron Density: The TaiWan Ionospheric Model (TWIM)

- Approach : vertical α-Chapman layers + 2D surface spherical harmonics fitting

$$N_e(\theta,\lambda,h)=\sum_{i=1}^{n} N_{e\max}(\theta,\lambda)\times e^{\frac{1}{2}\left(1-\frac{h-h_m(\theta,\lambda)}{H(\theta,\lambda)}-e^{-\frac{h-h_m(\theta,\lambda)}{H(\theta,\lambda)}}\right)}$$

where n=6 for $F2_{top}$, $F2_{bottom}$, F1.5, F1, E, and D-layers, and the peak density (N_{emax}), peak height (h_m), and scale height (H) are combinations of surface spherical harmonics.

- Advantage: equivalent layers for physical layers; peak height and peak density for each physical layer are explicit parameters.

  Drawback: inaccuracy of fitting profiles.

Radio Science, 44, doi:10.1029/2009RS004154, 2009.

Comparisons between Chapman-layer fitting profiles (in blue) and RO N_e profiles (in red)

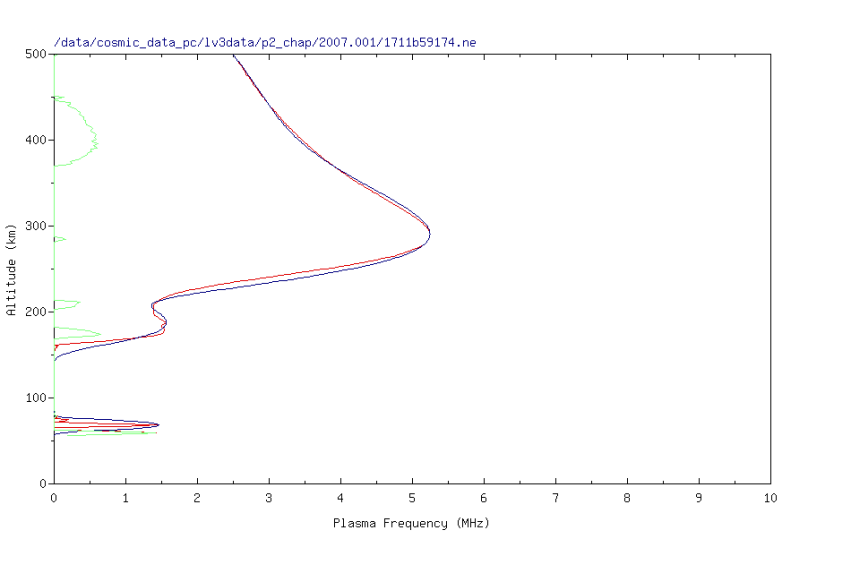

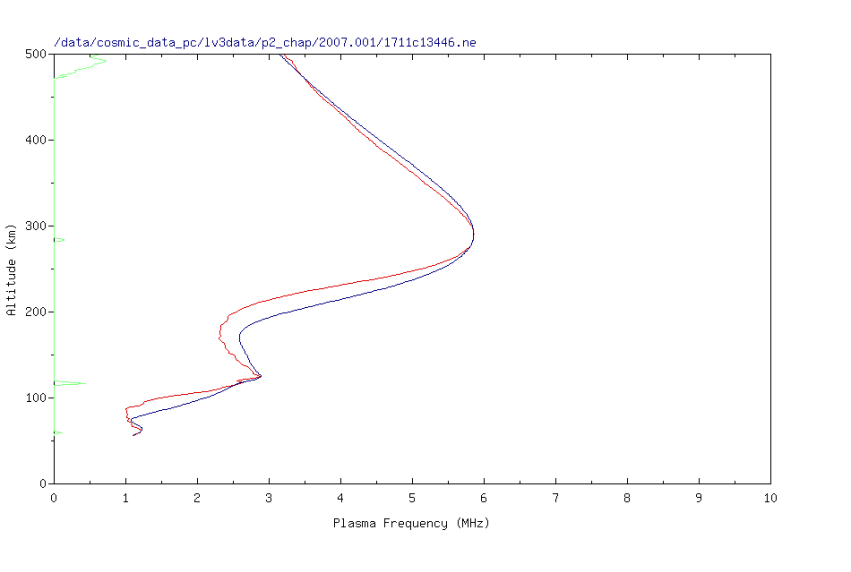

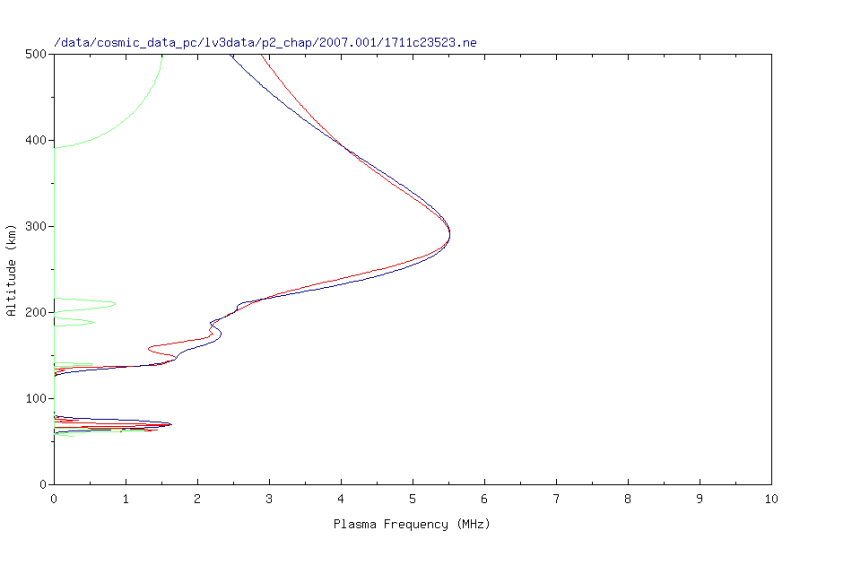

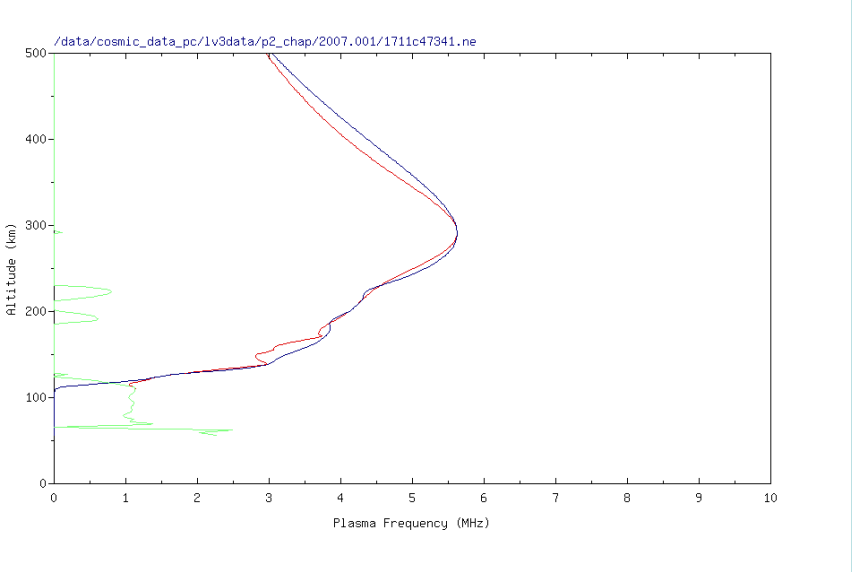

Numerical mapping of ionospheric parameters (e.g. *foF2* and *hmF2*) by the least squares method

- The spherical surface Laplace equation is

$$\frac{1}{\sin\theta}\frac{\partial}{\partial\theta}\left(\sin\theta\frac{\partial\Gamma}{\partial\theta}\right)+\frac{1}{\sin^2\theta}\frac{\partial^2\Gamma}{\partial\phi^2}=0\,.$$

- The resulting real and orthogonal functions are defined by

$$U_{nm}(\theta,\phi)=\sqrt{\frac{2n+1}{2\pi}\frac{(n-m)!}{(n+m)!}}\,P_n^m(\cos\theta)\cos m\phi\,,\ and$$

$$V_{nm}(\theta,\phi)=\sqrt{\frac{2n+1}{2\pi}\frac{(n-m)!}{(n+m)!}}\,P_n^m(\cos\theta)\sin m\phi\,,\ where\ n=0,1,2,\cdots,\ m=0,1,2,\cdots,n.$$

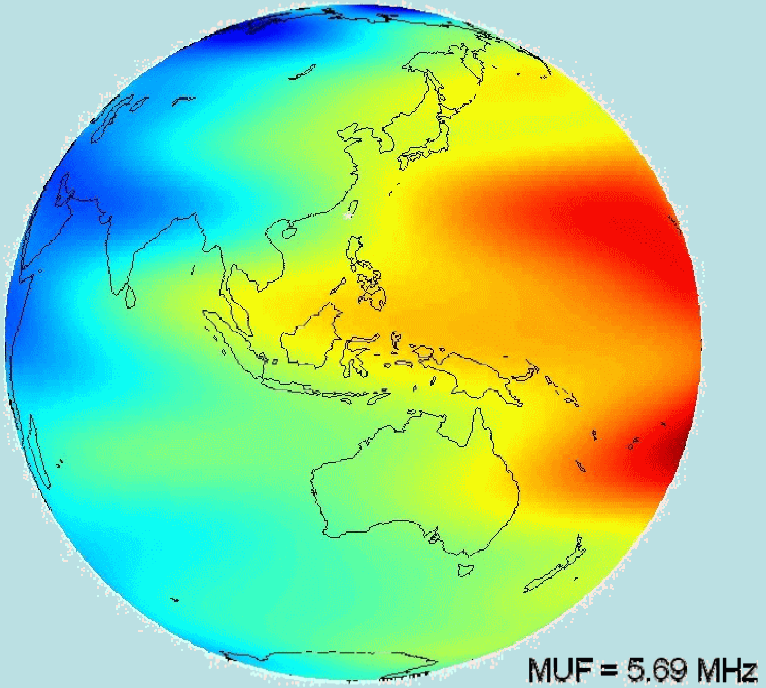

foF2 maps in UT

- Includes universal time (UT) and local time (LT) modes.

Evaluation of TWIM limb TEC by RO measurements

- The TEC ratio (TR) profile (between the calibrated path TEC and the simulated modeling path TEC) is defined:

$$TR(r) = \frac{TEC'(r)}{\int_{P_1}^{P_2'} N_e^{TWIM}(r,\theta,\lambda)\, dl}.$$

- Examples of TR profiles on the 95th day in 2008:

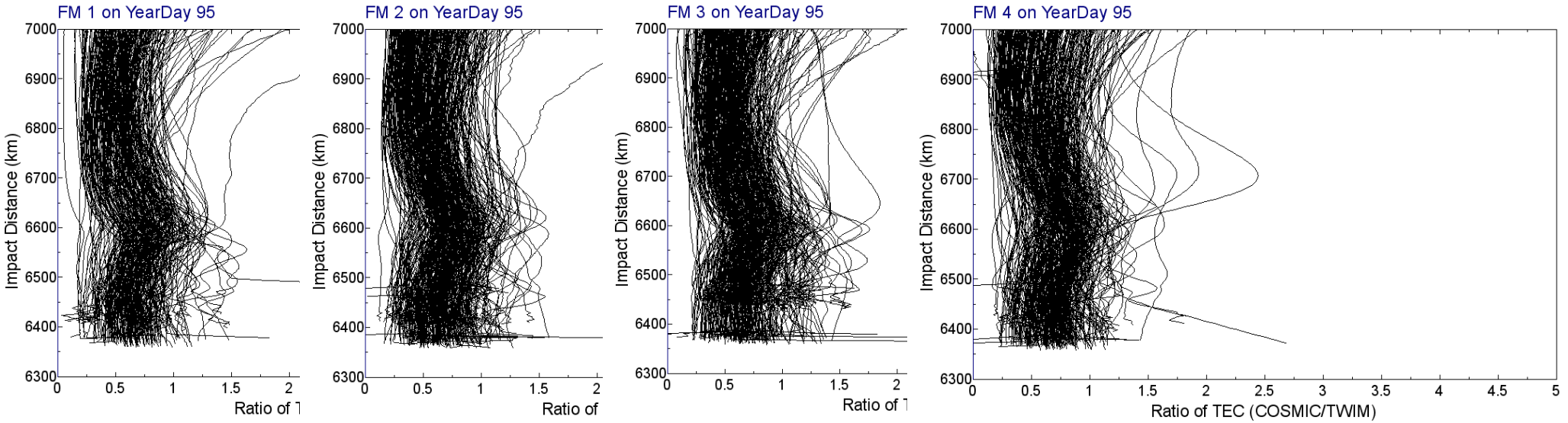

Evaluation of TWIM vertical TEC by JASON data

- Evaluated by JASON vTEC data (from April 2007 to Dec. 2009).
- The mean vTEC difference are ~ -2 TECU. The *rms* vTEC differences are ~4.5 TECU.
- Examples on the 86th day in 2008:

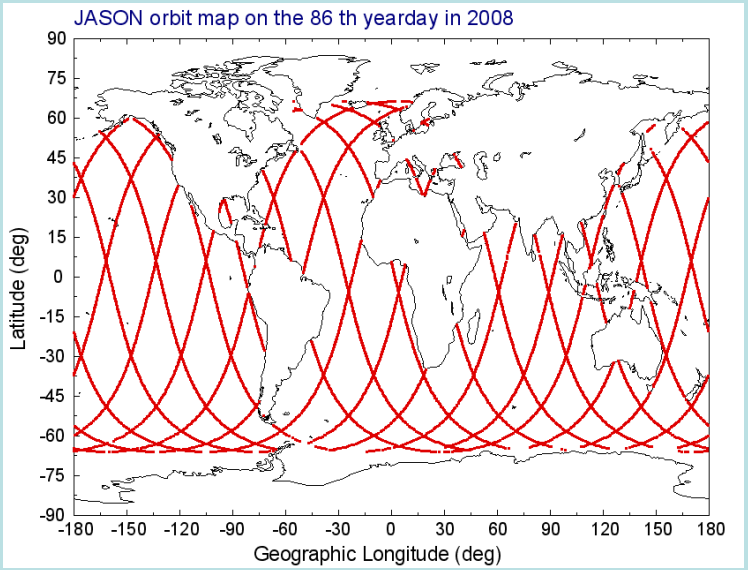

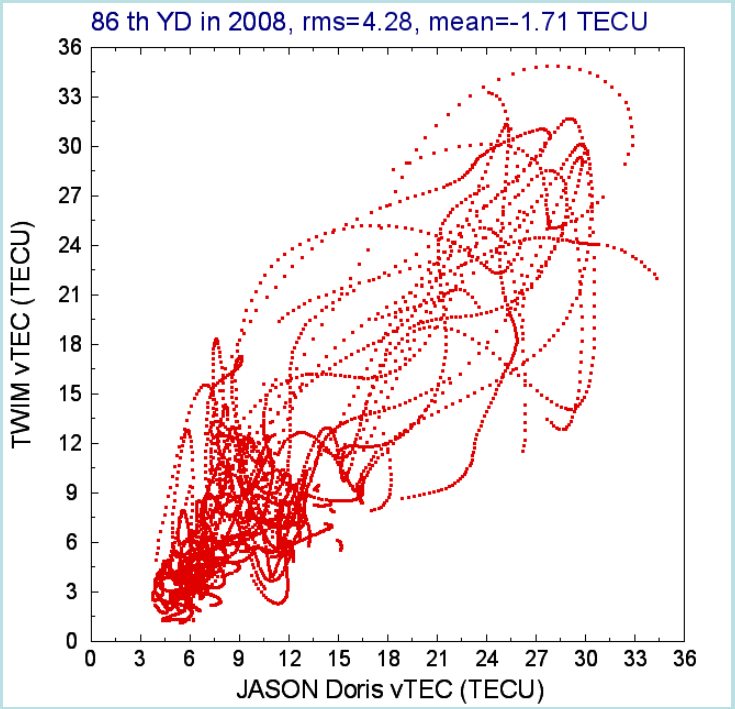

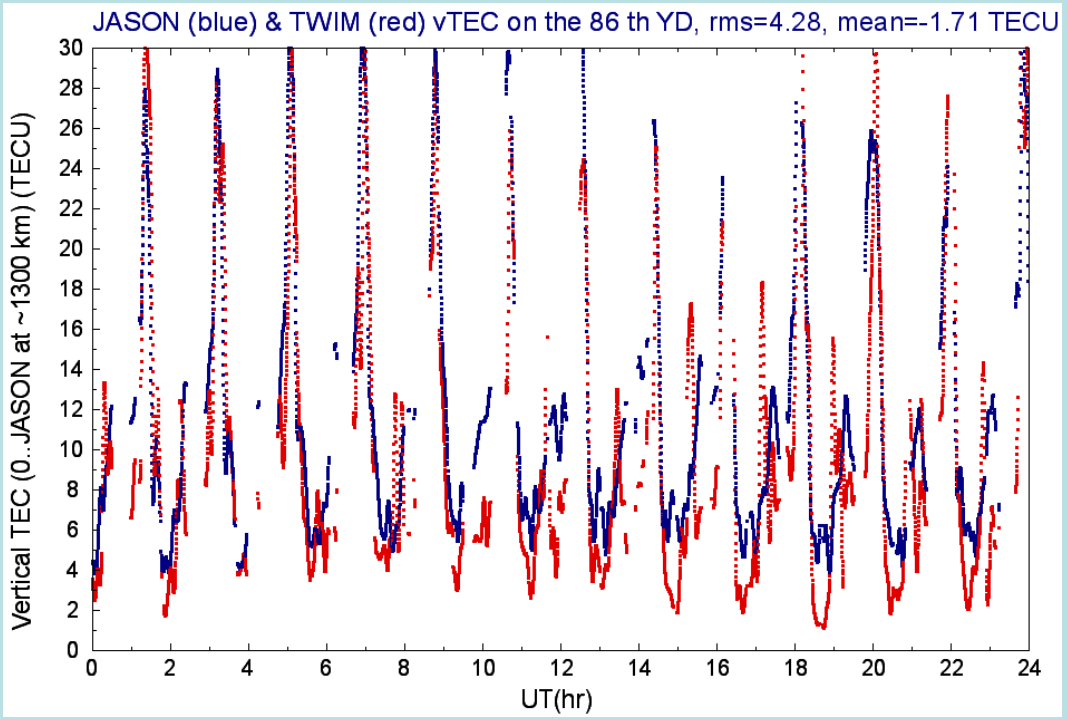

March, June, September, and December noontime *foF2* maps (from top to bottom)

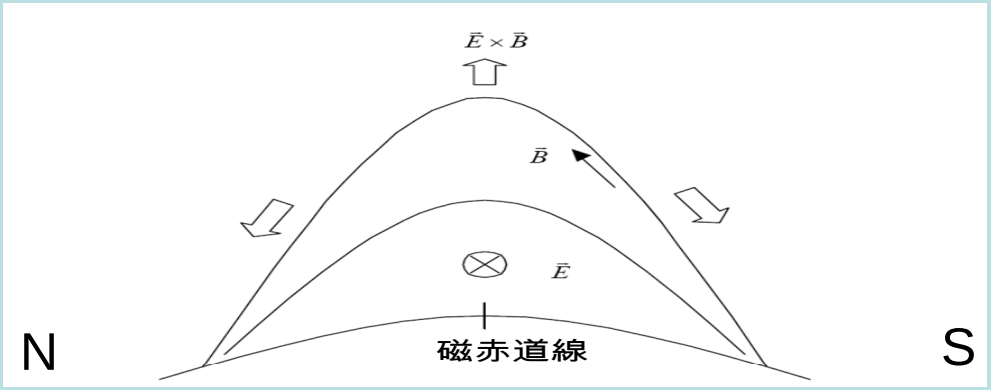

1. The June noontime *foF2* map shows that the north-pole area has higher values (~5 MHz) than the south-pole area (~2 MHz), which is in continuous night during the winter.
2. All the noontime *foF2* maps show one equatorial N_e trough along the dip equator and two N_e crest traces at ±~18° magnetic dip latitudes for equatorial anomaly (EA).
3. For seasonal variations of EA at noon, the *foF2* values along the two crests are highest at the March equinox and lowest at the June solstice.

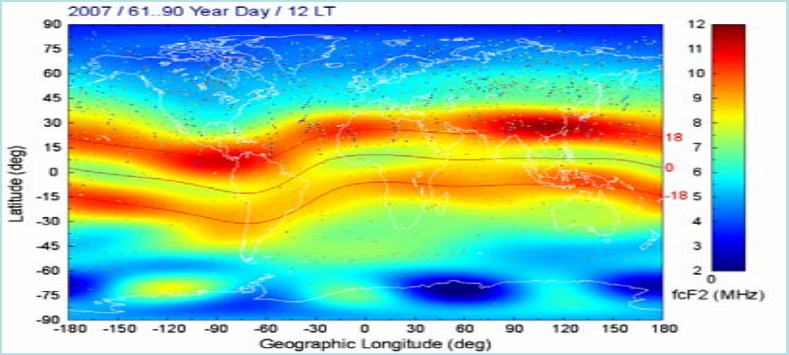

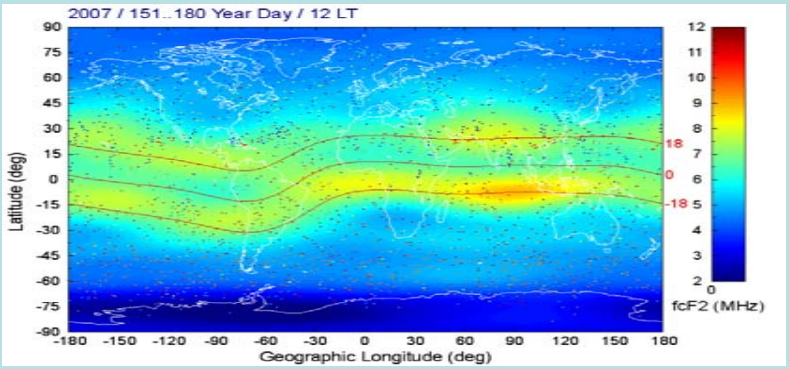

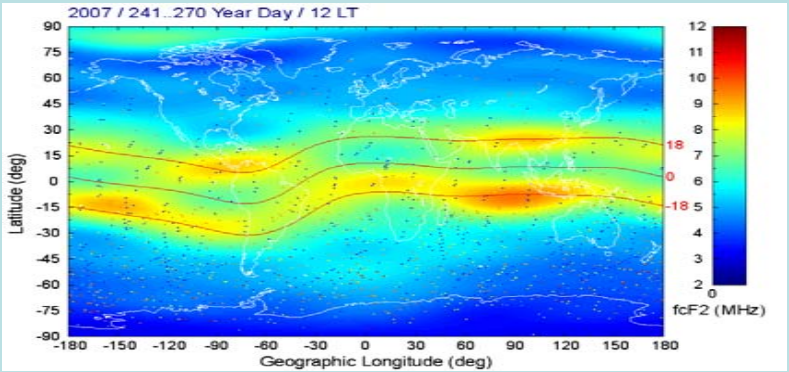

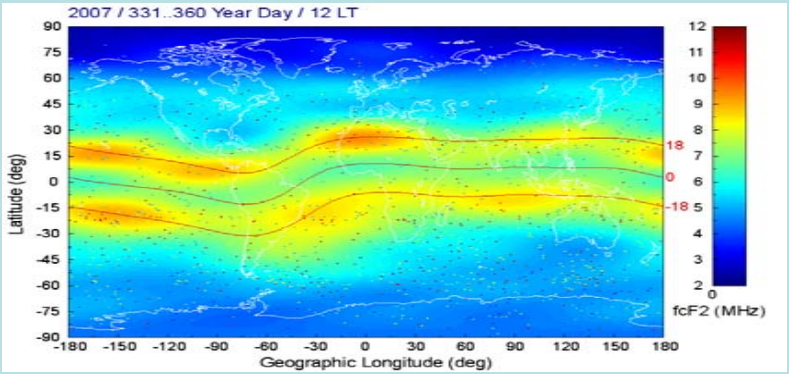

March, June, September, and December noontime *hmF2* maps (from top to bottom)

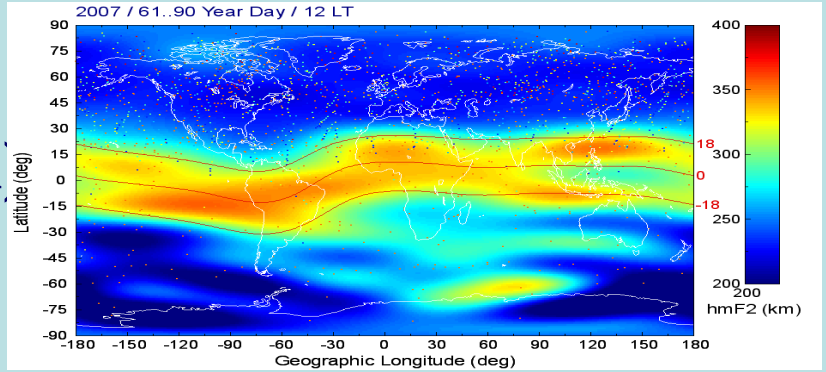

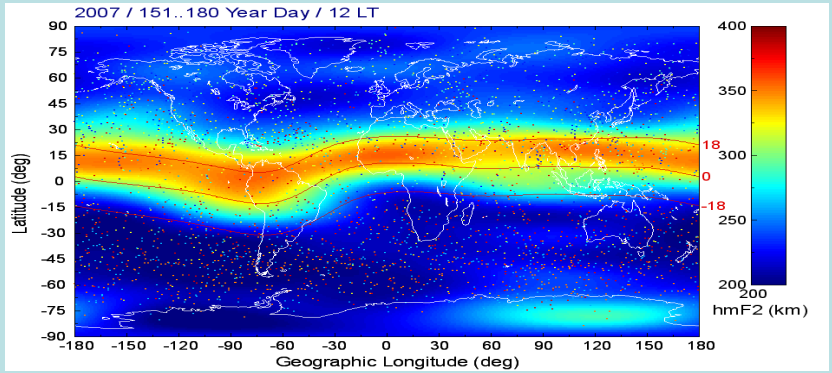

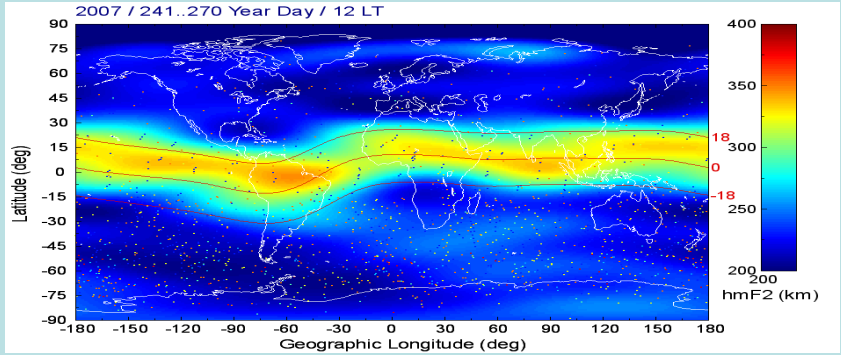

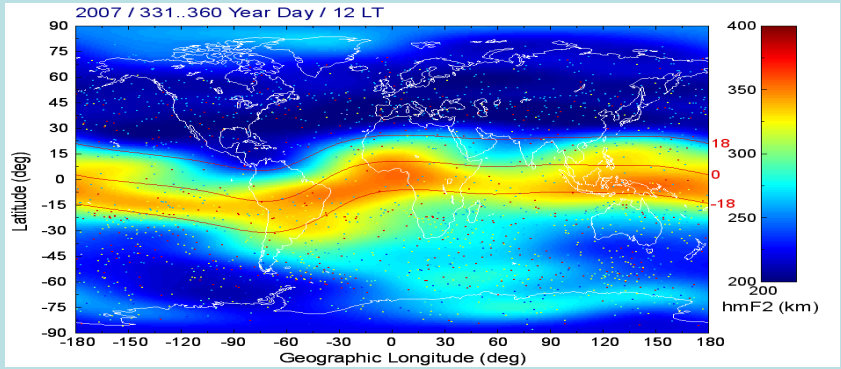

1. From the June noontime *hmF2* map the mid- and high-latitude *hmF2*s in the northern hemisphere generally have relatively higher values (by 30-40 km) than the southern hemisphere.
2. Summer-to-winter wind effects can transport plasma up the field line and produce higher *hmF2*s in the northern hemisphere and low dip latitude regions, as shown in the June *hmF2* maps; there are lower *hmF2*s in the southern hemisphere and low dip latitude regions vice versa.

March, June, September, and December noontime *HF2* maps (from top to bottom)

1. The June noontime *HF2* map shows that the mid- and high-latitude *HF2*s in the northern hemisphere generally have relatively thicker values (by 10-20 km) than the southern hemisphere.
2. Summer-to-winter wind effects can also transport plasma up the field line and produce thicker *HF2*s in the northern hemisphere and low dip latitude regions, as shown in the June *HF2* maps; there are lower *HF2*s in the southern hemisphere and low dip latitude regions vice versa.
3. The noontime *HF2* values display peaks along the dip equator and are largest in March and lowest in June.
4. For seasonal variations of EA at noon, the *HF2* values along the dip equator are highest at the March equinox and lowest at the June solstice.

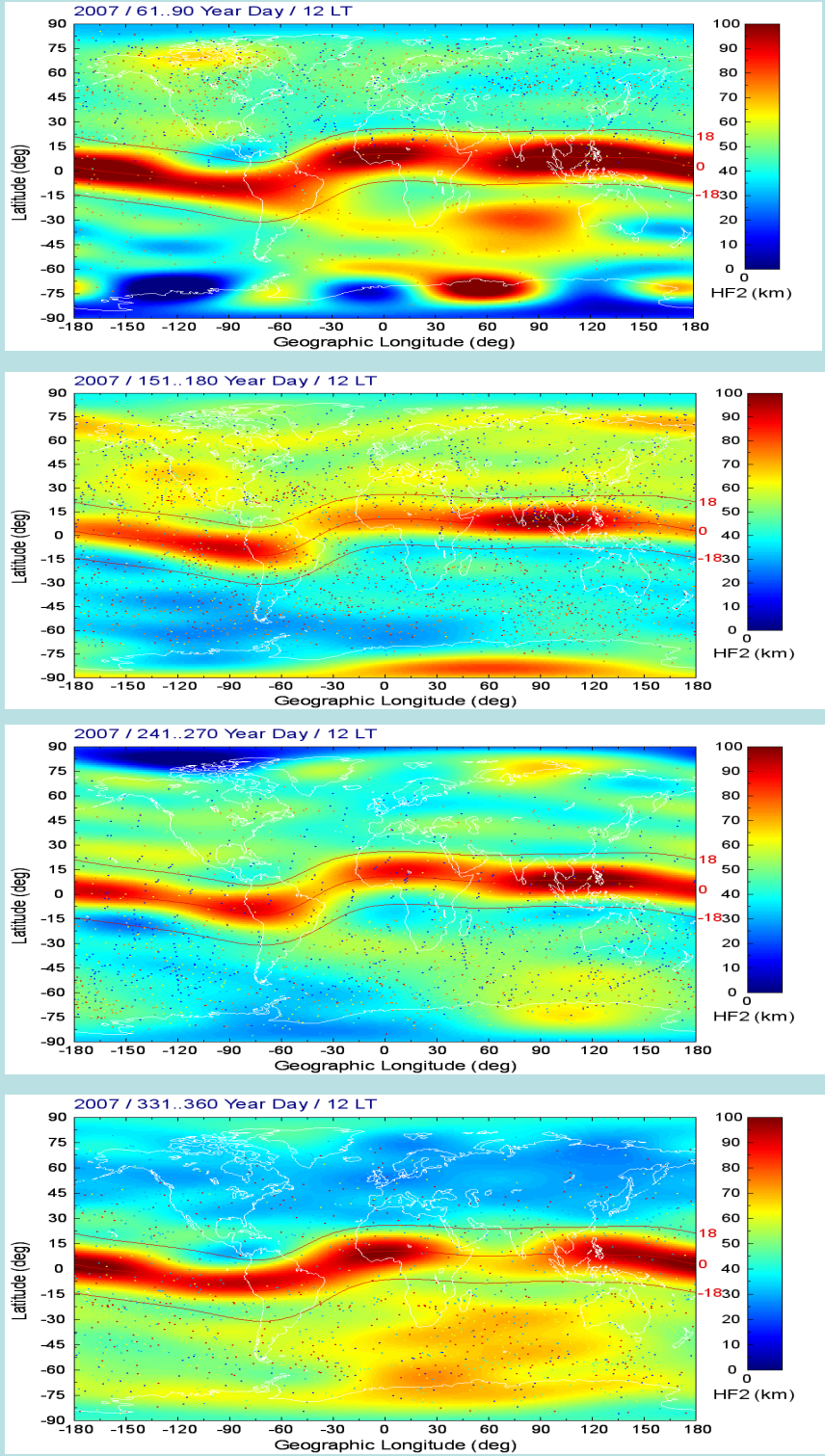

Validation of compensated TEC retrieved *foF2* and *foE* by the ionosonde data

- Evaluated by ionosonde data (49 stations) from days 81~180 in 2008.
- ~4000 matches out of ~150,000 RO observations.

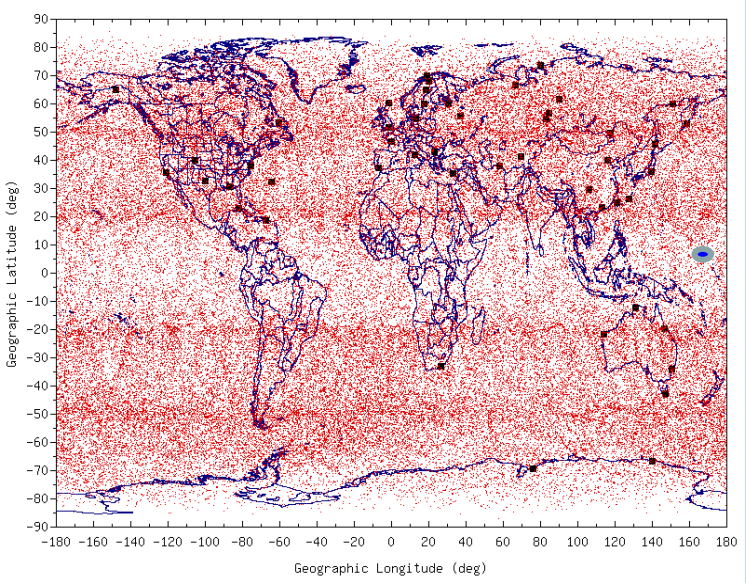

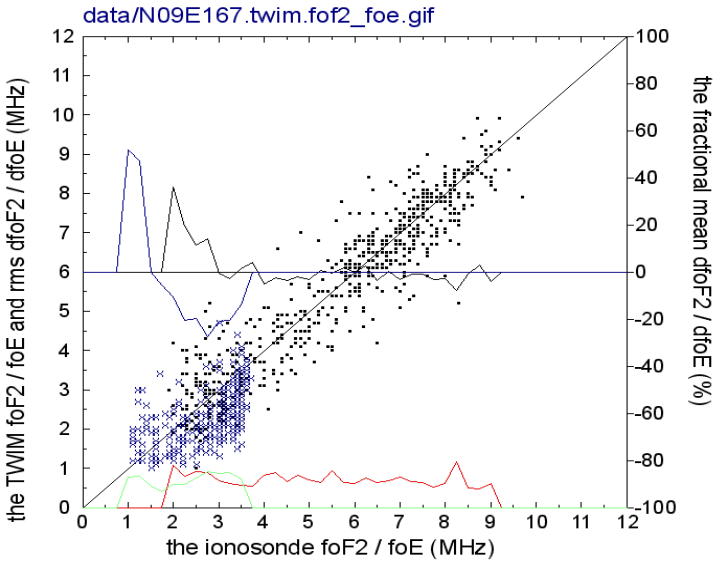

- mean (rms) *foF2* difference = -0.12 (0.76) MHz
  mean (rms) *foE* difference = -0.37 (0.94) MHz
- The mean d*foF2*s are ≦0.5 MHz averagely and ≦0.25 MHz from 0° to 60° dip-latitude region.
- The retrieved *foE* values are underestimated and typically worse at the southern hemisphere.

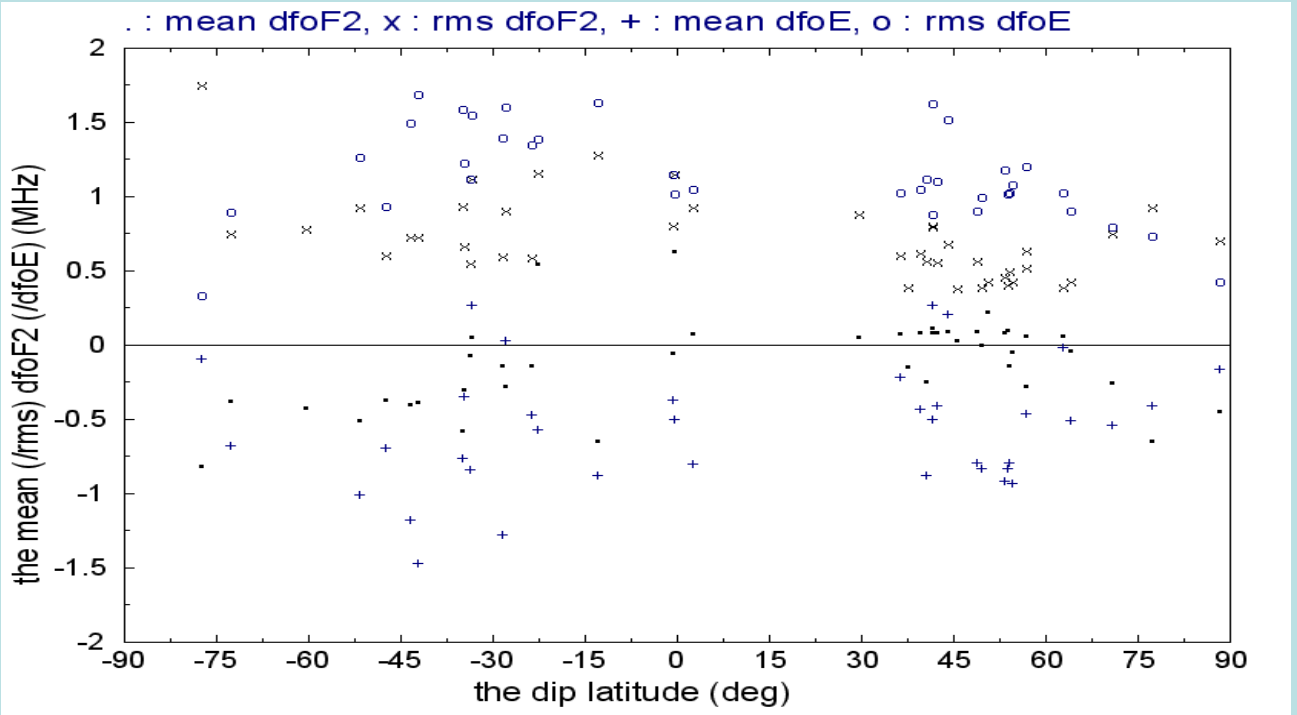

Final remarks

- FormoSat-3/COSMIC has become a promising program for monitoring the large-scale global ionosphere.

- A 3D approach using vertical Chapman layers and surface spherical harmonics for modeling variations of ionospheric Ne have been proposed and implemented to be the TaiWan Ionospheric Model (TWIM).

- The standard Abel inversion error because of potential horizontal gradient and inhomogeneities of the ionosphere could be reduced by compensating path TECs based on a qualified ionospheric model, e.g, TWIM.

Future works

- Including ionosonde and ISR measurements to improve the TWIM results.